

# High-pressure cation-exchange treatment of a ZSM-5 zeolite

Aijie Han

*Department of Chemistry, University of Texas–Pan America, Edinburg, Texas 78539*

Yu Qiao<sup>a)</sup>

*Department of Structural Engineering, University of California at San Diego, La Jolla, California 92093-0085*

(Received 11 February 2009; accepted 20 April 2009)

Under ambient pressure, an aqueous solution may not enter the nanopores of a hydrophobic ZSM-5 zeolite, which imposes difficulties to cation-exchange treatment. In the current study, a high-pressure cation-exchange technique is developed. With a relatively short treatment time, the degree of hydrophobicity is significantly increased.

## I. INTRODUCTION

ZSM-5 zeolite is an aluminosilicate that usually has a high silica-to-alumina ratio.<sup>1–5</sup> It contains two sets of nanopores. One set of nanopores is straight, with the cross-sectional size of  $5.3 \times 5.6 \text{ \AA}$ ; the other set is S-shaped, with the cross-sectional size of  $5.2 \times 5.5 \text{ \AA}$ .<sup>6</sup> An Al atom at the center of an  $\text{AlO}_4$  tetrahedron connects to adjacent  $\text{SiO}_4$  tetrahedron by sharing an O atom and thus generates a negative framework charge counterbalanced by extra-framework cations, such as alkaline or alkaline-earth cations.

If the alumina content is relatively high, the nanopore surface can be acidic.<sup>7–9</sup> Such ZSM-5 zeolites are chemically reactive and/or catalytically active, having been widely applied for hydrocarbon interconversion, catalysis, etc. Often, the as-synthesized ZSM-5 zeolites need to be further modified to control the properties of inner surfaces of nanopores, such as the degree of hydrophobicity. For instance, for active liquid spring or programmable catalysis, the liquid infiltration needs to be controlled by an external pressure, and the working pressure must be adjusted in an appropriate range.<sup>10–14</sup> One commonly used technique is cation-exchange.<sup>15–17</sup> As H-form zeolite crystals are immersed in an aqueous solution of electrolyte, cations can diffuse into the network. The framework defect sites can be effectively deactivated. Consequently, the nanopore walls become more nonpolar and less wettable to water; i.e., the effective degree of hydrophobicity increases. For a highly hydrophobic zeolite, however, the ordinary cation-exchange treatment can be relatively inefficient because the electrolyte solution does not enter the nanopores spontaneously, and thus the cation-exchange only takes place at positions close to the pore opening and the

process can be relatively slow. A promising alternative for introducing transition metal cations into extra-framework positions of zeolites is the solid-state ion-exchange technique.<sup>18–20</sup> However, the process usually demands high vacuum or with inert gas protection.<sup>21,22</sup>

## II. EXPERIMENTAL

In the current study, a ZSM-5 zeolite with a silica-to-alumina ratio of 280 was investigated. The synthesis mixture was prepared by adding to deionized water at room temperature: tetraethoxysilane [(TEOS) 98%; Sigma-Aldrich, St. Louis, MO], aluminum isopropoxide (98%; Sigma-Aldrich), and tetrapropylammonium bromide [(TPABr) 98%; Sigma-Aldrich] at the molar ratio of TPABr:TEOS:Al[OCH(CH<sub>3</sub>)<sub>2</sub>]<sub>3</sub>:H<sub>2</sub>O = 0.08:1:0.0036:80. The mixture was stirred at room temperature for 30 min, and then ammonium fluoride [(NH<sub>4</sub>F) 98%; Sigma-Aldrich] was introduced under vigorous stirring. The molar content of NH<sub>4</sub>F was the same as that of silica. The mixture was homogenized and aged for 3 h, and then poured into an autoclave and hydrothermally treated at 200 °C for 48 h, after which white powders of as-synthesized ZSM-5 crystals were formed. The crystalline material was filtered, washed with deionized water, and dried at 120 °C. Finally, it was calcined in a tube furnace at 550 °C for 2.5 h in air.<sup>23</sup>

The calcined ZSM-5 zeolite was examined by x-ray diffraction. The result indicated that the material was well crystallized. The cation-exchange treated samples were obtained by immersing 0.5 g of ZSM-5 crystals in a 7 g of liquid phase under atmospheric pressure for 12 h at 95 °C. The temperature was controlled by a water bath. The liquid phase was a saturated aqueous solution of either sodium chloride (26.4%) or sodium nitrate (46.7%). The treated ZSM-5 zeolite was washed repeatedly by deionized water, filtered, and dried in air.

Figure 1 depicts the high-pressure treatment system. A milk-like suspension was produced by dispersing 0.5 g

<sup>a)</sup>Address all correspondence to this author.

e-mail: yqiao@ucsd.edu  
DOI: 10.1557/JMR.2009.0285

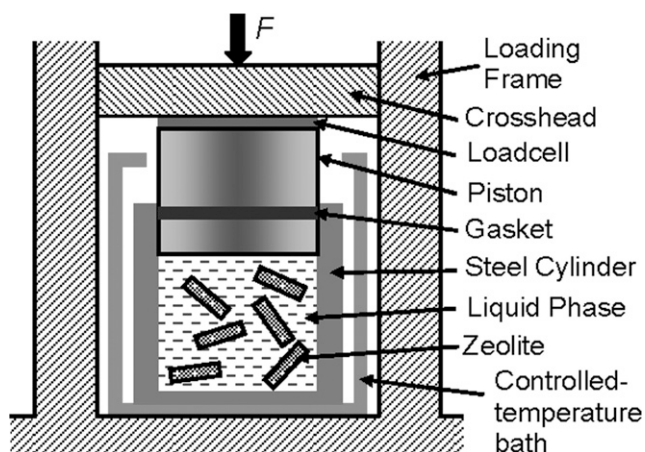


FIG. 1. A schematic diagram of the high-pressure cation-exchange treatment system.

of ZSM-5 zeolite in 7 g of saturated NaCl or NaNO<sub>3</sub> solution. The suspension was sealed in a stainless steel cylinder. By moving the cross-head of a type 5582 Instron machine (Instron, Norwood, MA) downward, a quasi-hydrostatic pressure was applied on the liquid phase through a piston. The piston was sealed by a gasket consisting of two reinforced polyurethane O-rings. The axial load,  $F$ , was measured by a 50 kN loadcell, and the pressure was assessed as  $F/A_0$ , where  $A_0 = 286 \text{ mm}^2$  was the cross-sectional area of the piston. The pressure was maintained at 140 MPa for 3 h. The treatment temperature was kept constant at 95 °C by a thermal bath. After 12 h, the cation-exchanged zeolite was washed by deionized water and dried in air.

The degree of hydrophobicity of the inner nanopore surface was directly characterized by a pressure-induced infiltration experiment. The testing setup was similar with Fig. 1. A suspension of 0.4 g of cation-exchange-treated ZSM-5 zeolite and 3 g of deionized water was sealed in the steel cylinder. At room temperature, the piston was compressed into the cylinder at a constant rate of 0.5 mm/min. As the pressure exceeded approximately 150 MPa, the piston was moved out at the same rate. The sorption-isotherm curves are shown in Fig. 2. Because no significant difference in infiltration/defiltration could be detected for the samples treated by NaCl and NaNO<sub>3</sub> solutions, only the results of the NaCl-modified system are shown.

### III. RESULTS AND DISCUSSION

In Fig. 2, it can be seen clearly that even without any cation-exchange treatment, the synthesized ZSM-5 zeolite is highly hydrophobic. By thermal motion, a limited number of H<sub>2</sub>O molecules may randomly overcome the energy barrier and infiltrate into the open end of nanopores; however, defiltration is much easier than further moving deep into the nanopore. As an H<sub>2</sub>O molecule

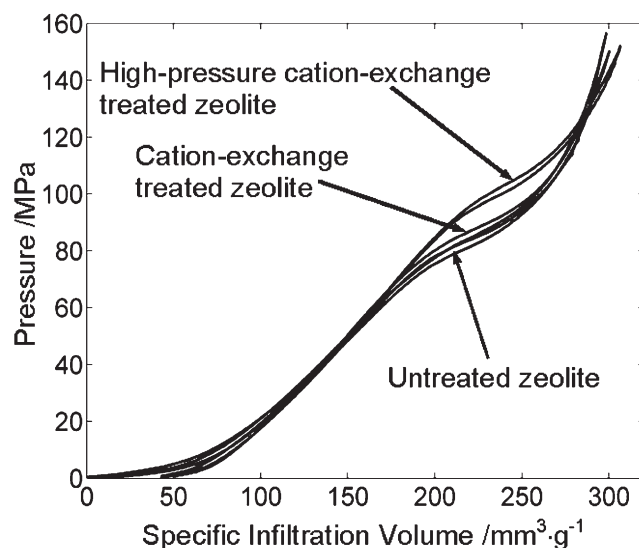


FIG. 2. Typical high-pressure sorption isotherm curves.

enters a nanopore, it must overcome the energy barrier from hydrogen bonds with surrounding H<sub>2</sub>O molecules and establish the high-energy, unstable interaction with a nanopore wall. The energy associated with the former process may be assessed as one third of the evaporation energy of water, which is approximately 2.2 kJ/g or  $6.6 \times 10^{-20} \text{ J}$  per molecule.<sup>24</sup> If the characteristic molecular size and distance are taken as 2 and 4 Å, respectively, an external pressure of  $p_1 = 20 \text{ MPa}$  should be applied to balance the energy barrier. The external pressure required to overcome the excess solid-liquid interfacial tension may be estimated as  $p_2 = 2\Delta\gamma/r$ , where  $\Delta\gamma \approx 10 \text{ mJ/m}^2$  and  $r \approx 0.3 \text{ nm}$  is the effective nanopore radius.<sup>25</sup> Thus,  $p_2 \approx 67 \text{ MPa}$ . Consequently, as the pressure reaches  $p_{cr} = p_1 + p_2 = 87 \text{ MPa}$ , the elastic energy in the bulk liquid phase outside the nanopores is higher than the increase in system free energy associated with liquid infiltration; that is, it is energetically favorable for the liquid molecules to enter the nanopores to release the quasi-hydrostatic pressure. As the liquid infiltrates, the system volume decreases significantly with a small pressure increment, causing the formation of the infiltration plateau. When the nanopores are filled, the pressure-induced infiltration stops, and the system compressibility decreases rapidly, converging back to the bulk modulus of water. It is clear that the high degree of hydrophobicity of the ZSM-5 zeolite with high silica-to-alumina ratio results in the high infiltration pressure. Note that the definition of hydrophobicity in the liquid infiltration experiment is different from that in a gas adsorption test, where no liquid phase is involved. In general, for gas adsorption, when the silica-to-alumina ratio of a zeolite is higher than 18, the material can be regarded as hydrophobic. For liquid infiltration, the silica-to-silica ratio must be much higher.

As the pressure is reduced to below  $p_{cr}$ , the external pressure becomes insufficient to keep the liquid inside the nanopores. Since the free energy outside nanopores is smaller than inside, water molecules tend to diffuse out of the nanoenvironment. Around  $p_{cr}$ , as the pressure decreases slightly, most of the confined liquid defiltrates, resulting in the defiltration plateau. As the external pressure further decreases, because the nanopores have already been empty, the system behavior is dominated by the bulk liquid phase. The defiltration plateau is nearly identical to the infiltration plateau, indicating that the liquid infiltration and defiltration process is reversible.

As the hydrophobic ZSM-5 zeolite crystals are immersed in an electrolyte solution, the sodium cations enter the nanopores and exchange with the proton. That is, the nanopore wall becomes less polar. Because water molecules are polar, the zeolite tends to be more hydrophobic. Under ambient pressure, it is energetically unfavorable for water molecules to enter the hydrophobic nanopores, which suppresses the conventional ion-exchange process in aqueous solution. As shown in Fig. 2, after the material is treated for 12 h, the infiltration pressure indeed increases. However, the change in  $p_{cr}$  is small, only approximately 2% from 87 to 89 MPa. It is clear that the exchange and diffusion of cations are quite slow, even when the treatment temperature, 95 °C, is relatively high. This result may be attributed to the following: before the cation-exchange treatment, the zeolite is already highly hydrophobic; and under ambient pressure, the liquid phase cannot enter the nanopores, and, thus, only the outer crystal surfaces can be exposed to the cations. Because cation-exchange treatment is critical to zeolite chemistry, a large number of research efforts on thermodynamics and kinetics of cation-exchange of natural zeolites has been reported,<sup>26</sup> whereas theoretical and experimental work on high-pressure cation-exchange is still in its early stage. In the current study, the crystal size of zeolite is 10 to 20  $\mu\text{m}$ . The specific BET surface area is approximately 400  $\text{m}^2/\text{g}$ , and the pore volume is approximately 0.15  $\text{cm}^3/\text{g}$ , according to a gas adsorption analysis by using Micromeritics TriStar 3000 Analyzer (Micromeritics, Norcross, GA). The effects of the porosity properties, such as pore size and pore volume, are still somewhat inadequately understood. The details of ion transport and ion-exchange processes may be better understood via parameterized study in computer simulation, which will be one of the focuses of future work.

During the high-pressure treatment experiment, the pressure in the bulk liquid phase is much higher than  $p_{cr}$ . Therefore, the electrolyte solution is forced into the nanopores, leading to the large solid-liquid contact area. Note that the morphology of the zeolite crystals is stable as long as the pressure is lower than 500 MPa. Because

the pressure is quasi-hydrostatic, it should not have a pronounced influence on the diffusion of cations between confined and bulk liquid phases. As the cation-exchange between the solid and liquid phases takes place over the nanopore surface, the exchange rate is largely increased. When the remaining defect sites are neutralized, the degree of hydrophobicity approaches the upper limit. As a result, after a relatively short treatment, the infiltration pressure increases by 15 from 87 MPa, approximately 17% of  $p_{cr}$  of the untreated sample.

The anion specie does not have any detectable effect on the result of the high-pressure cation-exchange treatment. As NaCl is changed to  $\text{NaNO}_3$ , no variation in infiltration pressure of treated samples is observed, as it should be, because anions are often inactive compared with cations. The difference in mass percentage concentration of NaCl and  $\text{NaNO}_3$  does not cause much variation in infiltration pressure, probably because the cation-exchange effect has been saturated.

#### IV. CONCLUDING REMARKS

In summary, because electrolyte solution does not spontaneously infiltrate into highly hydrophobic ZSM-5 zeolite crystals, variation in degree of hydrophobicity cannot be modified efficiently through ordinary cation-exchange treatment. By applying a quasi-static pressure higher than the infiltration pressure, the electrolyte solution can be forced into the nanopores. Under this condition, the cation-exchange can occur over the large nanopore surface, largely increasing the surface reaction rate. The treatment result is quite independent of the anion specie.

#### ACKNOWLEDGMENT

This work was supported by The National Science Foundation under Grant No. CBET-0754802.

#### REFERENCES

1. G.T. Kokotailo, S.L. Lawton, D.H. Olson, and W.M. Meier: Structure of synthetic zeolite ZSM-5. *Nature* **272**, 437 (1978).
2. D.H. Olson, G.T. Kokotailo, S.L. Lawton, and W.M. Meier: Crystal structure and structure-related properties of ZSM-5. *J. Phys. Chem.* **85**, 2238 (1981).
3. R.J. Argauer, M.D. Kensington, G.R. Landolt, and N.J. Audubon: *Crystalline Zeolite ZSM-5 and Method of Preparing the Same*. U.S. Patent No. 3702886, Mobil Co. (1972).
4. J.C. Lin and K.J. Chao: Distribution of silicon-to-aluminium ratios in zeolite ZSM-5. *J. Chem. Soc., Faraday Trans. 1* **82**, 2645 (1986).
5. A.T. Bell: NMR applied to zeolite synthesis. *Colloids Surf., A: Physicochem. Eng. Aspect.* **158**, 221 (1999).
6. Ch. Baerlocher, L.B. McCusker, and D.H. Olson: *Atlas of Zeolite Framework Types*, 6th Ed. (Elsevier, Amsterdam, 2007).
7. H. van Koningsveld: *Compendium of Zeolite Framework Types* (Elsevier, Amsterdam, 2007).

8. M. Hunger, D. Freude, D. Fenzke, and H. Pfeifer: H-1 solid-state NMR-studies of the geometry of bronsted acid sites in zeolites H-ZSM-5. *Chem. Phys. Lett.* **191**, 391 (1992).
9. E. Bourgeatlamy, P. Massiani, F. Direnzo, P. Espiau, F. Fajula, and T.D. Courieres: Study of the state of aluminum in zeolite-beta. *Appl. Catal.* **72**, 139 (1991).
10. Y. Qiao, G. Cao, and X. Chen: Effects of gas molecules on nanofluidic behaviors. *J. Am. Chem. Soc.* **129**, 2355 (2007).
11. A. Han and Y. Qiao: Infiltration pressure of a nanoporous liquid spring modified by an electrolyte. *J. Mater. Res.* **22**, 644 (2007).
12. A. Han and Y. Qiao: Thermal effects on infiltration of a solubility-sensitive volume memory liquid. *Philos. Mag. Lett.* **87**, 25 (2007).
13. A. Han and Y. Qiao: Pressure induced infiltration of aqueous solutions of multiple promoters in a nanoporous silica. *J. Am. Chem. Soc.* **128**, 10348 (2006).
14. Y. Qiao, V.K. Punyamurtula, A. Han, X. Kong, and F.B. Surani: Temperature dependence of working pressure of a nanoporous liquid spring. *Appl. Phys. Lett.* **89**, 251905 (2006).
15. R.T. Pabalan and F.P. Bertetti: Cation-exchange properties natural zeolites, in *Natural Zeolites: Occurrence, Properties, Applications, Reviews in Mineralogy and Geochemistry*, vol. 45, edited by D.L. Bish and D.W. Ming (The Mineralogical Society America and the Geochemical Society, 2001).
16. D. Caputo and F. Pepe: Experiments and data processing of ion exchange equilibria involving Italian natural zeolites: A review. *Microporous Mesoporous Mater.* **105**, 222 (2007).
17. P.S. Neuhoff and L.S. Ruhl: Mechanisms and geochemical significance of Si-Al substitution in zeolite solid solutions. *Chem. Geol.* **225**, 373 (2006).
18. H.G. Karge and H.K. Beyer: *Solid-State Ion-Exchange in Microporous and Mesoporous Materials* (Springer, 2002).
19. A.V. Kucherov and A.A. Slinkin: Introduction of transition metal ions in cationic positions of high-silica zeolites by a solid state reaction. Interaction of copper compounds with H-mordenite or H-ZSM-5. *Zeolites* **6**, 175 (1986).
20. H.K. Beyer, H.G. Karge, and C. Borbely: Solid-state ion exchange in zeolites: Part I. Alkaline chlorides/ZSM-5. *Zeolites* **8**, 79 (1988).
21. A. Seidel, G. Kampf, A. Schmidt, and B. Boddenberg: Zeolite ZnY catalysts prepared by solid-state ion exchange. *Catal. Lett.* **51**, 213 (1998).
22. M.A. Zanjanchi and A. Ebrahimian: Studies on the solid-state ion exchange of nickel ions into zeolites using DRS technique. *J. Mol. Struct.* **693**, 211 (2004).
23. B. Louis and L. Kiwi-Minsker: Synthesis of ZSM-5 zeolite in fluoride media: An innovative approach to tailor both crystal size and acidity. *Microporous Mesoporous Mater.* **74**, 171 (2004).
24. D.R. Lide: *CRC Handbook of Chemistry and Physics* (CRC Press, 2007).
25. S. Hartland: *Surface and Interface Tension* (CRC Press, 2004).
26. *Reviews in Mineralogy and Geochemistry*, edited by D.L. Bish and D.W. Ming (Mineralogical Society of America and the Geochemical Society, Washington, DC, 2001), pp. 452–518.